1992A&A...254..198B

Astron. Astrophys. 254, 198–212 (1992)

ASTRONOMY AND ASTROPHYSICS

On the decay of the magnetic fields of single radio pulsars

Dipankar Bhattacharya[1,2,3,*], **Ralph A.M.J. Wijers**[1,2,3], **Jan Willem Hartman**[4], **and Frank Verbunt**[1,3,4]

[1] Institute for Theoretical Physics, University of California, Santa Barbara, CA 93106, USA
[2] Astronomical Institute 'Anton Pannekoek', University of Amsterdam, Kruislaan 403, NL-1098 SJ Amsterdam, the Netherlands
[3] Center for High-Energy Astrophysics, NIKHEF-H, Kruislaan 409, NL-1098 SJ Amsterdam, the Netherlands
[4] Institute of Astronomy, University of Utrecht, Postbox 80000, NL-3508 TA Utrecht, the Netherlands

Received August 2, accepted October 5, 1991

Abstract. We investigate the statistical evidence for the decay of the magnetic field of single radio pulsars. We perform population syntheses for different assumed values for the time scale of field decay using a Monte Carlo method. We allow for the selection effects in pulsar surveys and compare the synthesized populations with the observed pulsars. We take account of the finite scale height of the distribution in the Galaxy of free electrons, which determine the dispersion measure and hence the apparent distance of radio pulsars. Our simulations give much better agreement with the observations if the time scale for the field decay is assumed to be longer than the typical active life time of a radio pulsar. This indicates that no significant field decay occurs in single radio pulsars.

Key words: interstellar medium:general – pulsars: general – pulsars: magnetic field – pulsars: population statistics – stars: magnetic field – stars: neutron

1. Introduction

From the early days of pulsar astronomy, statistical studies of the pulsar population have been used to probe the evolution of pulsars. Much discussion in the literature has been devoted to the derivation of the properties of pulsars at birth, and to the estimation of pulsar birth rate (Gunn & Ostriker 1970, Taylor & Manchester 1977, Phinney & Blandford 1981, Vivekanand & Narayan 1981, Lyne et al. 1985, Chevalier & Emmering 1986, Stollman 1987, Narayan 1987, Emmering & Chevalier 1989, Narayan & Ostriker 1990). These different studies differ in the treatment of selection effects in pulsar surveys and in assumptions about the luminosity distribution of pulsars, but most of them assume that the magnetic-field strengths of neutron stars decay exponentially with a time constant of $\lesssim 10^7$ yr.

It has, however, been pointed out by several authors that the decay of magnetic fields of neutron stars is a shaky proposition. On theoretical grounds, Baym, Pethick & Pines (1969) argued that the interior of a neutron star is expected to be very highly conducting, and any magnetic field will be trapped there for ever. Computations by Sang & Chanmugam (1987) showed that even if the magnetic flux is confined only to the crust of a neutron star, ohmic decay in $\lesssim 10^7$ yr time scale would be difficult to understand.

Of late, observational evidence has also been mounting against quick decay of neutron star magnetic fields (see Bhattacharya 1991, Bhattacharya & Srinivasan 1991, Bhattacharya & Van den Heuvel 1991 for reviews). Existence of old neutron stars with substantial field strengths such as Her X-1, PSR 0655+64, millisecond pulsars, radio pulsars in globular clusters, and gamma-ray burst sources clearly indicate that the magnetic field of these neutron stars are not decaying significantly. The often-quoted evidence in favour of magnetic-field decay in isolated (non-binary) radio pulsars, namely the discrepancy between the kinetic ages and the spindown ages of neutron stars (Lyne et al. 1982,1985), was marginal to begin with, and has practically disappeared with the availability of a larger number of pulsar velocity measurements (Bailes 1989, Harrison et al. 1991).

In view of these developments, new models of the evolution of the magnetic fields of neutron stars have been proposed, which associate magnetic-field decay with the evolution of the neutron star in presence of a close binary companion (Shibazaki et al. 1989, Srinivasan et al. 1990, Romani 1990). According to these models, little or no field decay of isolated neutron stars is expected to occur.

Is this expectation consistent with the observed properties of the pulsar population? This is the question we address in the present paper.

We interpret the spindown torque on the pulsar $P\dot{P}$ as a direct measure of the magnetic field strength (see Eq. 2). It has been argued that a decay of the spindown torque may occur due to reasons other than the decay of the magnetic field strength, such as a secular evolution of the angle between the spin axis and the magnetic dipole (e.g. Kundt 1988, Blair & Candy 1989, Beskin et al. 1984). We wish to emphasize that our treatment adresses the issue of the evolution of the spindown torque as a whole, though we continue to refer to it as the evolution of the magnetic field strength for the sake of convenience.

Some earlier studies have already noted that the statistical properties of the pulsar population may be consistent with long field decay time scales (Krishnamohan 1987, Fokker 1987), or a power-law field decay (Sang & Chanmugam 1990). These studies do not model the selection effects in pulsar surveys satisfactorily, and discuss only the distribution of periods and period derivatives of pulsars, without attempting to fit other observable properties of the population. A case in point is the distribution of pulsars

Send offprint requests to: Frank Verbunt, Utrecht
*On leave from Raman Research Institute, Bangalore, India

© European Southern Observatory • Provided by the NASA Astrophysics Data System

1992A&A...254..198B

as a function of the height z above the galactic plane. The large velocities that pulsars are observed to have ($\langle v_z \rangle \sim 110$ km s^{-1}, see Lyne et al. 1982, Cordes 1986, Harrison et al. 1991) carry them to $z \sim$ several kpc before they significantly decelerate and return towards the plane. A short ($\lesssim 10^7$) yr time scale for magnetic-field decay will, however, so severely restrict the radio-active life time of a pulsar that the distribution of *functioning pulsars* would not extend beyond $z \sim 1$ kpc. The longer the field decay time scale, the more extended will the average life time of pulsars be, and hence the more wide will be their z-distribution. The issue of magnetic-field decay of pulsars thus cannot be treated in isolation from that of their z-distribution.

The fact that the z-distribution of pulsars, derived from their dispersion measures (column density of free electrons in the line of sight), does not extend beyond ~ 1 kpc has often been thought to be due to short active life times of pulsars as a result of magnetic-field decay. However, as pointed out by Bhattacharya & Verbunt (1991), the finite thickness of the distribution of electrons that determine the dispersion measure causes the distances of pulsars at $z \gtrsim 1$ kpc to be systematically underestimated, and thus the true z-distribution of pulsars may be more extended than the derived one. In their extensive statistical study Narayan & Ostriker (1990), however, accept the derived z-values of pulsars at their face value, and find evidence for a second population of pulsars born at $z > 400$ pc. This result may well be an artifact of underestimated z-distances of an extended tail of the pulsar population. Keeping this in mind, we assume in this paper that pulsars form a *single* population, and investigate the nature of the *apparent* z-distribution for different values of the field decay time scale.

In the present analysis we take recourse to Monte Carlo methods to generate an artificial population of pulsars, at a constant birth rate, with certain assumed properties at birth. We follow the evolution of each pulsar, and its motion in the Galaxy, up to a specified epoch of observation. From these, we construct a subsample which would meet the fiducial detection criteria in four major pulsar surveys, and will also be beamed towards the observer. The properties of this subsample are then compared with those of the sample of observed pulsars.

Our approach is similar to that adopted by Emmering & Chevalier (1989), but we have made several important improvements. Instead of assuming that pulsars move with constant velocity, we have taken into account the gravitational potential of the Galaxy in their dynamics. Further, we have taken care to be as internally consistent in our approach as possible. For example, among the known pulsars we have retained for comparison with our simulated sample only those which meet exactly the same detection criteria as we use for the simulated sample. This point has been ignored by Emmering & Chevalier (1989), and most other studies of pulsar statistics so far made.

The dispersion measures of the simulated pulsars were computed from an adopted model of the distribution of free electrons in the Galaxy. To be consistent with the observed dispersion measures of pulsars in globular clusters, and the distances of pulsars determined from HI observations and parallax measurements, we had to make several modifications to the existing model (Lyne et al. 1985) of the electron density distribution. We then revised the distance estimates of observed pulsars according to this electron density model, and used these revised distances in our final analysis.

2. Simulation and detection of a pulsar population

To compare a simulated sample of radio pulsars with the observed sample, we proceed in three steps. First, we simulate a population of radio pulsars in an area around the Sun. Next we determine which of these pulsars would have been detected by any of four surveys. And finally, we compare the simulated detections with the actual detections of the same surveys. These three steps are described in the following three subsections.

2.1. Simulation of a pulsar population

In simulating the pulsar population, we make assumptions about the properties of radio pulsars at birth, and then let these properties evolve for each pulsar separately. The parameters for each simulation are those which specify the properties at birth plus those that determine the evolution. The relevant properties of the individual pulsars and their relation to the simulation parameters are as follows.

age t. We assume that the pulsar birth rate has not changed with time. In our simulation we therefore choose an age for each pulsar from a flat distribution between zero and the Hubble time. In practice, an upper limit to the pulsar age of three to five times the time scale for magnetic-field decay suffices as an upper limit to the ages allowed, because all pulsars older than this would have evolved beyond the death line in all our simulations (see below).

magnetic-field strength B. The initial magnetic-field strength B_i is chosen from a Gaussian distribution in $\log B_i$:

$$p(\log B_i)\, \mathrm{d}(\log B_i) = \frac{1}{\sqrt{2\pi}\sigma_B} \exp\left(-\frac{1}{2}\left[\frac{\log B_i - \log B_0}{\sigma_B}\right]^2\right) \mathrm{d}(\log B_i). \quad (1)$$

The field is assumed to be related to the pulse period P of the pulsar and its time derivative $\dot{P}$ according to (see Gunn & Ostriker 1970)

$$P\dot{P} = \frac{8\pi^2 R^6}{3Ic^3} B^2, \quad (2)$$

where R and I are the radius and the moment of inertia of the neutron star, respectively. We use the values $R = 10^6$cm and $I = 10^{45}$ g cm^2. We assume that the field decays exponentially according to

$$B(t) = B_i \exp(-t/\tau), \quad (3)$$

where τ is the time scale for the decay.

rotation period P. We assume an initial period which is the same for each pulsar, viz. $P_i = 0.1$ s. This period evolves, according to Eqs. (1 – 3) as

$$P^2 = P_i^2 + \frac{8\pi^2 R^6}{3Ic^3} B_i^2 \tau [1 - \exp(-\frac{2t}{\tau})]. \quad (4)$$

Pulsars that are born with periods shorter than P_i evolve to P_i on a time scale which is negligible with respect to the evolutionary time scales for the pulsar population that we consider. Our assumption for the initial fields therefore merely states that all pulsars are born with initial periods $P_i < 0.1$ s.

© European Southern Observatory • Provided by the NASA Astrophysics Data System

1992A&A...254..198B

beaming fraction f_b. The pulsar beam may or may not intersect the line of sight towards the Earth. The fraction f_b of the sky swept by a pulsar's beam is not very well known. The conventional assumption of $f_b \simeq 20\%$ may be a good one for pulsars with spin period $P \sim 1$ s, but observations suggest that at short periods the beam widens (Lyne & Manchester 1988), and perhaps becomes elongated (Narayan & Vivekanand 1983). These effects cause f_b to rise to higher values at short periods. In the model of Narayan & Vivekanand (1983) f_b rises to almost unity at $P \lesssim 0.1$ s, while according to Lyne & Manchester (1988) f_b has a much shallower behaviour, rising to ~ 0.35 at $P \sim 0.1$ s. Given the uncertainties, we have decided to examine all three of the above cases.

In our simulations we use approximations to the dependence of the beaming on the pulse period. The beaming function as determined by Narayan & Vivekanand (1983) is well approximated with

$$f_{b,NV} \propto P^{-\frac{1}{2}}, \tag{5}$$

and that by Lyne & Manchester (1988) with

$$f_{b,LM} \propto P^{-\frac{1}{3}}, \tag{6}$$

for $P > 0.1$s. A recent study by Rankin (1990) also indicates that the beamwidth scales as $P^{-1/2}$.

height above the galactic plane z and velocity in the z-direction v_z. We choose the initial height z_i above the galactic plane for the radio pulsars from an exponential distribution

$$p(z_i)\,\mathrm{d}(z_i) = \frac{1}{2h}\exp(-\frac{|z_i|}{h})\,\mathrm{d}(z_i), \tag{7}$$

where h is the scale height of the pulsar progenitors, i.e. of the O and B stars (e.g. Mihalas & Binney 1981, Table 4-16). The sign of z_i is allowed to be positive or negative. The initial velocity in the direction perpendicular to the galactic plane $v_{z,i}$ is chosen from a Gaussian distribution

$$p(v_{z,i})\,\mathrm{d}(v_{z,i}) = \frac{1}{\sqrt{2\pi}\sigma_v}\exp(-\frac{1}{2}(\frac{v_{z,i}}{\sigma_v})^2)\,\mathrm{d}(v_{z,i}). \tag{8}$$

$v_{z,i}$ can be either positive or negative.

The acceleration in the vertical direction due to the galactic potential at the position of the Sun has been determined by Kuijken & Gilmore (1989a,b). From Table 6 of Kuijken & Gilmore (1989b), and Eqs.(39,40) of Kuijken & Gilmore (1989a) we write:

$$g_z = 1.04 \times 10^{-3}(\frac{1.26z}{\sqrt{z^2 + 0.18^2}} + 0.58z), \tag{9}$$

where g_z is in units of kpc/Myr^2 and z in kpc. We use this potential to evolve z and v_z from their initial values to their current values after a time t.

projected position in galactic disk (x, y). The position of the pulsar, as projected on the galactic plane, is chosen randomly in a circle around the Sun with a radius of 3 kpc. This means that we assume that the pulsar birth rate, as well as the vertical acceleration due to the galactic potential, do not vary over this circle. It further implies that the pulsars born in the circle but leaving it during their evolution have similar properties as those born outside the circle and entering it. The correctness of these assumptions is somewhat doubtful, but in the absence of secure information on them, we chose not to burden our simulation with additional parameters.

luminosity at 400 MHz L_{400}. The dependence of the radio luminosity of a pulsar on its spin period P and period derivative $\dot{P}$ is rather uncertain. Several models have been proposed over the years, but the scatter of the luminosities of the observed pulsars around that predicted by any available model is huge. In the present work we have used two of the commonly used luminosity models, and compared the results in these two cases separately with observations. Assuming a power-law dependence of the luminosity on P and $\dot{P}$, Proszyński & Przybycień (1984) obtained a fit which, after rounding off the exponents, has the form (Narayan 1987):

$$\log \langle L_{400}\rangle_o = 6.64 + \frac{1}{3}\log\frac{\dot{P}}{P^3}, \tag{10}$$

where $\langle L_{400}\rangle_o$ is the observed mean 400 MHz luminosity in units of mJy kpc^2 (the luminosity L of a pulsar is defined to be equal to Sd^2, where S is the time-averaged flux received from the pulsar and d is its distance from the Earth). Stollman (1986,1987) suggested that the radio luminosity of a pulsar is related to the voltage generated above the polar cap, which is proportional to B/P^2. Observations indicate a dependence of $\langle L_{400}\rangle_o$ on this parameter for pulsars with polar cap voltage below a certain critical value (Stollman 1986; Taylor & Stinebring 1986; Srinivasan 1989), while the luminosity law seems to reach a maximum above this critical voltage. According to the fit obtained by Stollman (1986):

$$\begin{aligned}\log \langle L_{400}\rangle_o &= (-10.05 \pm 0.84) + (0.98 \pm 0.03)\log\tfrac{B}{P^2}, \quad \log\tfrac{B}{P^2} \le 13\\ &= 2.71 \pm 0.60, \qquad\qquad \log\tfrac{B}{P^2} > 13.\end{aligned} \tag{11}$$

Both of these luminosity laws refer to the relation between the period, period derivative and the *mean* luminosity of the *observed* pulsars. It is to be expected, however, that the observed sample will be severely biased towards more luminous pulsars. This bias has been modelled by Narayan & Ostriker (1990), who find that the distribution ρ_L of the intrinsic luminosities around the mean observed luminosity can be modelled as

$$\rho_L(\lambda) = 0.5\lambda^2 e^{-\lambda}$$
$$\text{where } \lambda \equiv c\left(\log\frac{L_{400}}{\langle L_{400}\rangle_o} + b\right). \tag{12}$$

In this equation b and c are parameters whose values have been obtained from fits to the observed distribution by Narayan & Ostriker. If $\langle L_{400}\rangle_o$ is described with Eq. (10), the values are $b = 1.8$ and $c = 3.6$. For Eq. (11) we use $b = 2.0$ and $c = 3.0$.

For each simulation, we start by fixing the simulation parameters. These are: P_i, $\log B_0$, σ_B, the choice of beaming law, h, σ_v, and τ. From these, we determine the properties of the individual pulsars. We use Monte Carlo methods (Press et al. 1986, pp. 195, 203) to select the age of the pulsar from a flat distribution between zero and a maximum age, and an initial magnetic-field strength from the Gaussian distribution as in Eq. (1). The maximum age is set to 5τ for $\tau < 100$ Myr and to 3τ for $\tau \ge 100$ Myr. With the initial pulse period, we first check whether the evolved pulse period and magnetic-field strength, as found from Eqs. (4,1), place the radio pulsar above the death line (Ruderman & Sutherland 1975, Rawley et al. 1986), i.e. whether

© European Southern Observatory • Provided by the NASA Astrophysics Data System

1992A&A...254..198B

$$\frac{B}{P^2} > 0.17 \times 10^{12}\mathrm{G/s^2} \tag{13}$$

If this condition is not met, the neutron star is counted as not observable as a radio pulsar, and dropped from the rest of the simulation. We again use a Monte Carlo method to determine whether the pulsar beam intersects the Earth, using Eq. (5) or Eq. (6). If the beam does not intersect the Earth, the pulsar is dropped from the rest of the simulation.

Next, we select an initial height of the pulsar above the galactic plane from the exponential distribution of Eq. (7), and an initial velocity from the Gaussian distribution of Eq. (8), using Monte Carlo methods (Press et al. 1986, pp. 201, 203). We compute the current z and v_z from their initial values by using the acceleration of Eq. (9). We also assign the pulsar a random projected position (x, y) in a circle in the galactic plane, centered on the Sun and with a radius of 3 kpc.

From the pulse period and the period derivative (or, equivalently, the magnetic field), we calculate the mean observed luminosity $\langle L_{400}\rangle_o$, according to either Eq. (10) or Eq. (11). With a Monte Carlo method we then pick the ratio $L_{400}/\langle L_{400}\rangle_o$ of the actual intrinsic pulsar luminosity to this observed mean, on the basis of Eq. (12).

2.2. *Detection of the simulated pulsar population*

The large surveys in which most of the known pulsars have been discovered suffer from strong selection effects. To make a comparison of the properties of the simulated pulsars with those of the observed pulsar population we have therefore retained only those pulsars among the simulated sample which meet the detection criteria of one of four major pulsar surveys conducted at 400 MHz, namely, the Jodrell Bank survey (Davies et al. 1972), U Mass-Arecibo survey (Hulse & Taylor 1974), Second Molonglo survey (Manchester et al. 1978), and U Mass-NRAO survey (Damashek et al. 1978). The detection criteria we use are largely the same as in Narayan (1987).

The detectability of a pulsar depends on several factors:

1. The flux S of the pulsar, determined by its luminosity and its distance from the Earth.
2. The "broadening" of the pulse due to the propagation of the pulsar signal through interstellar plasma. There are two separate contributions to this broadening: (*a*) Due to the presence of irregularities in the interstellar electron density, the signal from the pulsar reaches us not only via the direct route, but is also scattered in from other directions. The signals coming via the scattered routes are, of course, delayed due to the extra lengths of path travelled. Added together, these signals therefore result in a pulse of a larger width than at the point of emission. (*b*) Dispersion in the interstellar plasma causes the pulse arrival times to become frequency dependent. The lower the frequency, the later the pulse arrives. Over the finite bandwidth of the detector this introduces a broadening of the pulse.
3. The finite time resolution (sampling) of the detector, which adds a further component to pulse smearing. The final width W of the broadened pulse can be written as (Narayan 1987):
$$W^2 = W_e^2 + \tau_{samp}^2 + \tau_{DM}^2 + \tau_{scatt}^2, \tag{14}$$
where W_e is the width of the unbroadened pulse, and the contributions to broadening are indicated by the subscripts.

While τ_{scatt} depends only on the distance to the pulsar and the character of electron turbulence on the way, τ_{DM} is determined by the dispersion measure DM, as well as the detector characteristics. For a given survey, τ_{DM} can be written as C_{DM}DM, where C_{DM} is a constant. Values for C_{DM} and τ_{samp} for the four pulsar surveys we use have been listed by Narayan (1987).

The minimum detectable flux S_{min} in a pulsar survey depends on the modulated fraction of the signal. For a width W of the broadened pulse, S_{min} is proportional to $[W/(P-W)]^{1/2}$ (Dewey et al. 1984). It is, however, customary to quote the survey flux limits S_0 for the case where smearing is negligible, i.e. $W \simeq W_e \ll P$. This quantity is proportional to $[W_e/P]^{1/2}$, and has been quoted by Narayan (1987) for the surveys in question (βS_0 in his notation). The value of S_{min} for a given pulsar would then be obtained from

$$S_{min} = S_0 \left(\frac{T_r + T_{sky}}{T_0}\right) \left[\frac{PW}{W_e(P-W)}\right]^{1/2}. \tag{15}$$

Following Dewey et al. (1984) and Narayan (1987), we have used an intrinsic duty cycle W_e/P of 4% for every pulsar. T_r is the receiver excess noise temperature for the particular survey, T_{sky} is the sky background temperature in the direction of the line of sight to the pulsar, and T_0 is a suitable normalization constant. We used the values of T_r and T_0 tabulated by Narayan (1987).

Following the procedure described in Section 2.1, we computed, for each simulated pulsar, the luminosity L_{400}, and hence its flux $S_{400} = L_{400}/(x^2+y^2+z^2)$, where (x, y, z) is the position of the pulsar in heliocentric coordinates. The smeared pulsewidth W was then computed from Eq. (14) using values for the dispersion measure DM and the scatter broadening τ_{scatt} for the pulsar. Our method for the determination of DM and τ_{scatt} for a simulated pulsar is described in Section 2.2.1. The galactic latitude l and longitude b of the pulsar were computed from its heliocentric coordinates, and the sky background temperature T_{sky} for this (l, b) was then obtained by interpolation from a table of 400 MHz background temperatures taken from the all sky survey of Haslam et al. (1982). Using the survey characteristics tabulated by Narayan (1987), we evaluated from Eq. (15) the value of S_{min} for the pulsar in each of the included surveys. We counted the pulsar as "detected" if $S_{400} \geq S_{min}$ in any survey that covered the pulsar's position in the sky.

2.2.1. Determination of dispersion and scattering

The interstellar medium severely restricts our ability to detect pulsars. Pulse broadening, both due to scattering and dispersion, strongly increases with dispersion measure; as a result, the distance at which a pulsar becomes undetectable can be much less than that expected from the extrapolation of its apparent brightness by a simple inverse square law. Selection effects on pulse period are introduced in this manner: pulsar visibility depends on the ratio between pulse broadening and pulse period, and thus short-period pulsars disappear from our view at lower dispersion measures, i.e. at smaller distances.

It is known that dispersion is caused by free electrons, and is simply proportional to the integrated column density thereof in our line of sight. Scattering is determined by the characteristics of turbulence in the same free-electron component of the interstellar medium. Unfortunately, we have hardly any quantitative information about these properties of the interstellar medium except through observations of radio pulsars. The properties of pulsars and of the interstellar medium that hampers their detection are therefore partly derived from the same observations, and cannot be determined fully independently.

© European Southern Observatory • Provided by the NASA Astrophysics Data System

1992A&A...254..198B

The dispersion measure. Of real pulsars, we know the dispersion measure from observation. To compare our simulated population with observations, we have to assign a dispersion measure to our simulated pulsars, given their position in the Galaxy. This is only possible if we first estimate the distribution of free electrons in the Galaxy from observed pulsar dispersion measures. Observed pulsars with a good independent distance estimate are the best ones to use for this, but these are rare. In addition, one can use lower and upper limits to pulsar distances from HI absorption measurements.

Due to the clumpy nature of the interstellar medium, differences in average electron density of a factor of two between lines of sight only a few degrees apart on the sky are no exception. Combined with the paucity of independent pulsar distances, this makes deriving a model for the mean electron density a difficult task (and at the same time somewhat restricts the extent to which such a model is a meaningful representation of the real world), but it is the best we can do under the circumstances. We adopted the functional form for the dependence of the mean electron density on position in the Galaxy given by Lyne et al. (1985):

$$n_e(R,z) = \frac{1}{1+R/R_0}\left(n_1 e^{-|z|/H_1} + n_2 e^{-|z|/H_2}\right) + n_{GN}, \qquad (16)$$

in which R and z are galactocentric cylindrical co-ordinates, R_0 is the galactocentric radius of the Sun, and the subscripts 1 and 2 denote the contributions due to the thin and thick electron layer, respectively; n_{GN} is an extra contribution from the Gum Nebula. The parameter values of Lyne et al. (1985) are:

$$\begin{aligned} R_0 &= 10\,\text{kpc} \\ n_1 &= 0.015\,\text{cm}^{-3}\,; \quad H_1 = 70\,\text{pc} \\ n_2 &= 0.025\,\text{cm}^{-3}\,; \quad H_2 = \infty. \end{aligned} \qquad (17)$$

The Gum Nebula contribution is $0.28\,\text{cm}^{-3}$ inside a sphere of radius 115 parsecs, centered on a point located 0.5 kpc from the Sun in the direction ($\ell = 260°, b = 0°$), and zero outside that sphere (Lyne et al.1985).

We have changed these values in two ways: (*i*) the value of R_0 is set to 8.5 kpc, in agreement with more recent usage. Most distances used in estimating the electron density parameters are from HI measurements, and are therefore proportional to R_0 (see the compilation by Frail & Weisberg 1990). To make the predictions of DM for these pulsars (which were satisfactory in the old model) invariant under this change of R_0, we have to change $n_{1,2}$ by the inverse of the factor by which R_0 is changed (as DM has dimension distance times density). (*ii*) Now that many pulsars are known in globular clusters, far away from the galactic plane, it has become clear that the integrated column density perpendicular to the galactic plane is finite (Reynolds, 1989). Consequently, H_2 is finite; we adopt the value of Bhattacharya & Verbunt (1991) of 0.8 kpc. This value must be adapted to our change of n_2, because the quantity derived from observation is actually $n_2 H_2$. We therefore multiplied it by 0.85. We did not change the scale height of the thin layer or the Gum Nebula parameters (their observational determination does not involve R_0). Summarizing, we have used:

$$\begin{aligned} R_0 &= 8.5\,\text{kpc} \\ n_1 &= 0.0176\,\text{cm}^{-3} \quad H_1 = 70\,\text{pc} \\ n_2 &= 0.0294\,\text{cm}^{-3} \quad H_2 = 0.68\,\text{kpc}. \end{aligned} \qquad (18)$$

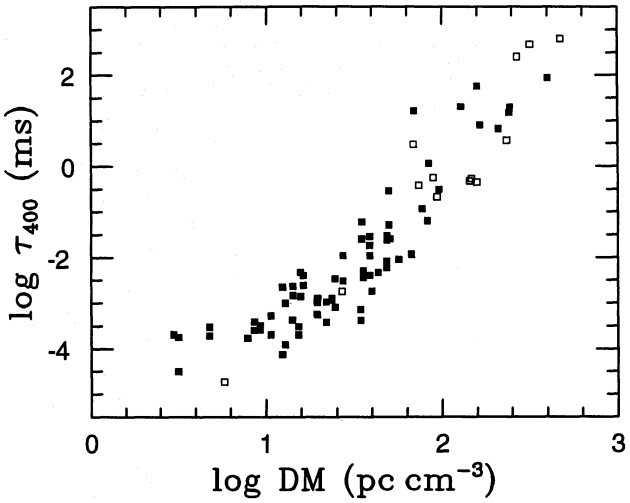

Fig. 1. Correlation between dispersion measure and scatter broadening time τ_{400} at 400 MHz. Open squares represent values scaled to 400 MHz from original measurements at frequencies outside the range 370–430 MHz

None of the numbers quoted actually has more than one significant digit, but we kept the extra digits in our numerical work to ensure that the results of the models only differ due to the difference in R_0. We then tested our model against the compilation of distances and dispersion measures of Frail & Weisberg (1990), and found no deviations between model predictions and data except for random scatter (of a factor of 1.5 r.m.s.).

We draw attention to an important consequence of a finite H_2: there is in this case a maximum model DM in each direction on the sky except exactly in the galactic plane. Some pulsars in lines of sight with above-average electron density have a greater DM than the maximum allowed by our mean electron model, and no model distance can be derived for them. This is the case for 24 radio pulsars in our compilation of 521; a further 38 are so close to the maximum that their derived distances are very sensitive to their value of DM (in the sense that a 10% change in their DM would result in more than 20% change of the derived distance; if H_2 were infinite, a 10% change in DM would always result in very nearly 10% change of the derived distance).

Scattering. Two methods have been used in previous work to find general expressions for the amount of scatter broadening of pulse profiles. Both rest on observations, but their approach is different. One method begins by noting that there is a strong correlation between observed DM and scatter broadening (Slee et al. 1980). We have plotted the data compiled by Cordes et al. (1985) in Fig. 1. (If in their list many measurents of one pulsar were listed, we only took the two extreme values measured closest to 400 MHz. Decorrelation bandwidths $\Delta\nu$ were converted to scattering times $\Delta\tau$ using $2\pi\Delta\nu\Delta\tau = 1$, and measurements at various frequencies were converted to 400 MHz by assuming that scattering times scale with observing wavelength λ as $\lambda^{4.4}$. For discussion of these points, see the paper by Cordes et al. (1985). Data points extrapolated from measurements outside the range 370 – 430 MHz are marked with open squares.) An empirical fit can now be made for τ_{400}, the scatter broadening time at 400 MHz observing frequency, as a function of DM. For a model pulsar, one then simply computes its τ_{400} from its model DM.

© European Southern Observatory • Provided by the NASA Astrophysics Data System

1992A&A...254..198B

The other method is to develop a theory of scattering in a turbulent interstellar medium, and fit a simple model for the distribution of scattering activity in the Galaxy. For a given simulated pulsar, τ_{400} is then computed from the model average scattering activity in the line of sight towards it. This method was adopted by Cordes et al. (1985) and Narayan (1987); we refer to these papers for a discussion of scattering models.

In Fig. 2, we present a comparison of two models with the data. In the left panel, differences between observed values of $\log \tau_{400}$ and those computed from the model of Narayan (1987) are plotted as a function of log DM. The right panel is a similar plot in which the model is a power law obtained by an unweighted least-squares fit to the data of Fig. 1. The error bars represent measurement uncertainties. As these are much less than the scatter in the data, that scatter must be largely intrinsic, which is why we fitted the power law model without weighting the data. Neither model is free from systematic trends of the residuals with DM. The Narayan fit predicts too much scattering more than twice as often as too little, and is almost always too much for $\mathrm{DM} < 50\,\mathrm{pc\,cm^{-3}}$.

The trend of the residuals in the simple power law fit is obviously due to the flattening of the correlation at low DM. It is thought that this flattening has a physical significance: at low DM, only scattering due to the diffuse interstellar medium plays a role, but at higher values of DM (and thus distance), our line of sight begins to intersect small, dense clumps of strongly scattering material. At high DM, these constitute the dominant contribution to the scattering. As we only seek a practical solution for estimating scattering, we shall remove the trend in the residuals by fitting a sum of two power laws to the data. This fit, and its residuals, are shown in Fig. 3. The best fit is

$$\tau_{400}[ms] = 10^{-4.62\pm0.52+(1.14\pm0.53)\log \mathrm{DM}} + 10^{-9.22\pm0.62+(4.46\pm0.33)\log \mathrm{DM}}. \quad (19)$$

The nominal best values of the fit parameters were used in the simulations to predict scattering from DM. It is seen that the residuals are free of trends.

Since the scatter around the mean is substantial, it may be of importance not to simply assign the best-fit model value of τ_{400} to a simulated pulsar, but randomly change that value in accordance with the observed distribution of residuals. This distribution is slightly skewed, and the cumulative distribution of residuals $\Delta \log \tau$ is represented very well by the function $(1 + \exp(\frac{x_0 - \Delta \log \tau}{a_0}))^{-1}$, with $x_0 = 0.040$ and $a_0 = 0.342$. It should be noted that for distances up to 3 kpc scattering is unimportant except for millisecond pulsars, which are not present in our sample.

2.3. The comparison sample of real pulsars

It is to be noted that the survey sensitivity limits used by us correspond to fluxes down to which the surveys were reasonably "complete", rather than the absolute minimum flux detected in them (see Narayan 1987 for a discussion). As a result, we cannot use *all* the real pulsars detected in these surveys to make a comparison with our simulations. We have therefore selected from the observed population those pulsars which meet exactly the same selection criteria as the "detected" pulsars in our simulated sample. For the real pulsars we used the *observed* values of S_{400} and DM, rather than computing them from the models mentioned above. Further, since our simulations generated pulsars within a heliocentric projected distance on the galactic plane d_{proj} of 3 kpc, we also applied this distance cutoff to the sample of real pulsars. These criteria led to the retention of 134 pulsars from the observed sample, 4 of which had to be further excluded from consideration since their period derivatives were not available to us.

5 of the 130 pulsars retained in our comparison sample have dispersion measures slightly above the maximum values that our electron density model predicts in their directions. As explained in Sect. 2.2.1, such a situation is expected to arise due to the clumpy nature of the interstellar medium, and strictly speaking, no model distance can be derived for these 5 pulsars. Nevertheless, we have chosen to retain them in our sample of pulsars with $d_{\mathrm{proj}} < 3$ kpc for the following reasons. First, their dispersion measures exceed the maximum value by only 4 to 17%, much less than the random variation of DMs between lines of sight ($\gtrsim 50\%$). Second, their relatively high latitudes make it unlikely that they are so far away that their d_{proj} exceed 3 kpc. Test calculations show that omission of these 5 pulsars from the comparison sample does not alter any of our conclusions.

3. Results

The number of parameters required to describe the pulsar population is rather large. Our interest in this paper is mainly in determining whether or not the observed properties of radio pulsars require a short decay time scale for the magnetic field. We have therefore fixed some of the parameters in our first simulations, in particular those which are not constrained very much by available observations. We thus fix the initial pulse period at $P_{\mathrm{i}} = 0.1$ s, the scale height of the progenitor population at $h = 0.06$ kpc, and the width of the initial velocity distribution at $\sigma_v = 110\,\mathrm{km\,s^{-1}}$. For the beaming law we choose Eq. (5) and for the luminosity Eqs. (10,12). The consequences of these choices, and of allowing variations therein, will be looked into in Section 3.3.

The simulation parameters that we allow to vary are the decay time τ, and the parameters $\log B_{\mathrm{i}}$ and σ_B of the distribution of the initial magnetic-field strengths, given by Eq. (1). In the following, we first discuss how we choose to compare the simulated pulsar samples with the real pulsars, and for which parameters the best solutions were found. We then proceed to compare the best solutions at short and long decay times, and investigate why the long decay times give better results.

3.1. Comparison of simulated and real pulsar distributions

For five different decay times, viz. 5, 10, 50, 100, and 300 Myr, we simulate a detected pulsar population for various combinations of $\log B_0$ and σ_B. Step sizes are 0.02 in $\log B_0$(G), and 0.01 in σ_B. Each simulated population is compared with the sample of 130 real pulsars that are detected according to the same criteria. The probability that the simulated population is equal to the real population was derived with the use of Kolmogorov-Smirnov tests, and of χ^2 tests.

For each simulated pulsar, a rather large number of parameters are determined with a Monte Carlo random procedure. A representative sampling of the allowed parameter space therefore requires a sufficiently large number of pulsars. For a number of pulsars that is too small, the probability as found from χ^2 and Kolmogorov-Smirnov tests may vary strongly with the seed first given to the random number generator. (Or, to put it

© European Southern Observatory • Provided by the NASA Astrophysics Data System

1992A&A...254..198B

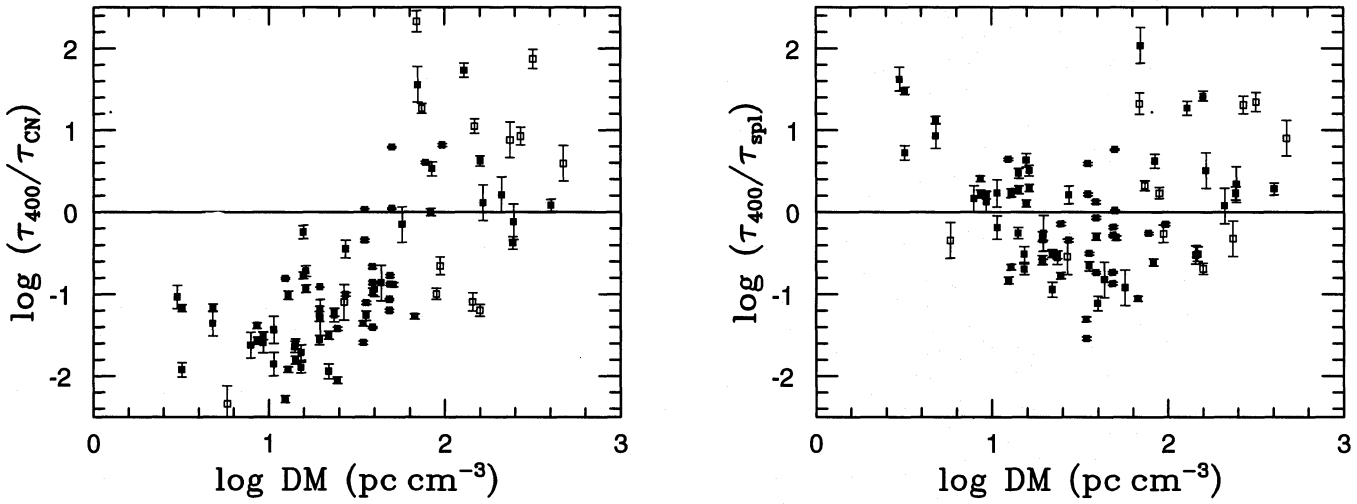

Fig. 2. Comparison of two scattering models. The ratio of τ_{400} to τ_{model} is plotted versus the dispersion measure. Error bars represent errors in τ_{400}. (*left*) Scattering times τ_{CN} from the model of Narayan (1987). (*right*) Model scattering times τ_{spl} from a single power-law fit to the data of Fig. 1

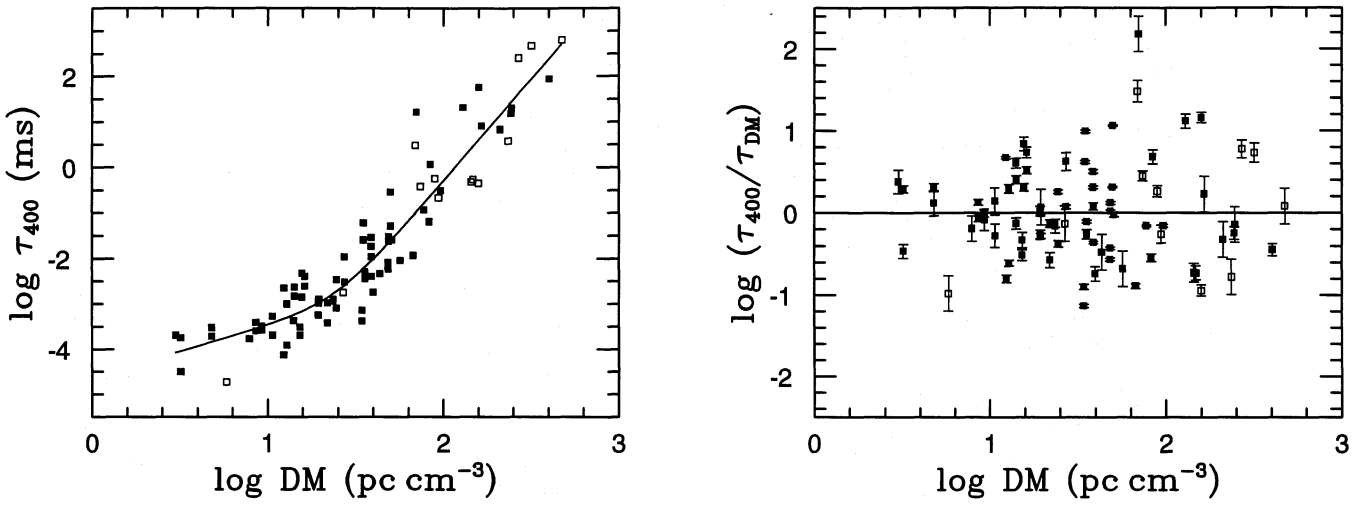

Fig. 3. Comparison between the scattering data and our fitted model τ_{DM} (a sum of two power laws). The residuals (*right panel*) are seen to be free of trends

the uncertainty in the derived probability is very large.) We therefore started by checking how many detected radio pulsars in our simulated sample were required to eliminate the influence of the value of the first seed number. On the basis of these tests, we decided to continue each simulation until 2000 pulsars were detected. For this number, only the third decimal of the logarithm of the probabilities that we calculate is affected by the original seed number.

We are not able to do two-sided χ^2 tests directly with the full sample of 2000 simulated pulsars, as these tests also check whether the number of pulsars in the simulated and real pulsar distributions are the same. We evade this problem by multiplying the number of simulated pulsars in each bin of the χ^2 tests with 130/2000. Because this procedure leads to artificially low Poisson noise in these bins, the probabilities found are between those of a genuine two-sided test and those of a one-sided test whether the real pulsars are sampled from the distribution of the simulated pulsars. The relative merits of fit are kept in order.

No such problem arises with the Kolmogorov-Smirnov tests, which can use the full sample of simulated detections. We decided therefore to search for the best solution using the K-S tests, and to use the χ^2 tests as a check.

For each simulated population, K-S tests and χ^2 tests (Press et al. 1986, pp. 475, 472) were done on the distributions of five pulsar properties, viz. the pulse period P, the magnetic field B, the characteristic age t_c, the "vertical component" of the dispersion measure $\mathrm{DM}\sin b$, and the luminosity (at 400 MHz) L_{400}. The bins used in the χ^2 tests are the same as those shown in Fig. 5, except for B, where the χ^2 tests use bins of 0.1 in $\log B$. If the probability provided by the K-S test is denoted Q, the probability that the simulated detections are from a similar distribution as the real detections is measured by the product of the separate probabilities. Our best solution for each decay time is defined as the one with a maximum value of the product $\Pi \equiv Q_P Q_B Q_{\mathrm{DM}\sin b} Q_L$, where the indices refer to the quantity tested in the K-S test. P and B are the two evolution parameters of the radio pulsar. $\mathrm{DM}\sin b$ was chosen as it represents the z-distribution, having the advantage over z itself of being an

© European Southern Observatory • Provided by the NASA Astrophysics Data System

1992A&A...254..198B

observable quantity. L_{400}, finally, tests the luminosity selection effects. A summary of the results is given in Table 1.

Table 1. Probabilities of the best simulations at a variety of parameters

τ(Myr)	$\log B_0$	σ_B	$\log \Pi$
	standard simulations		
5	12.54	0.32	-5.71
10	12.46	0.28	-3.04
50	12.36	0.29	-0.93
100	12.36	0.32	-0.56
300	12.32	0.32	-0.69
	Stollman luminosity law		
5	12.58	0.35	-5.16
10	12.46	0.30	-3.76
50	12.38	0.31	-1.94
100	12.38	0.33	-1.76
	$\sigma_v = 200$km/s		
10	12.46	0.29	-4.88
100	12.36	0.32	-2.87
	beaming Eq. (6)		
10	12.42	0.29	-2.12
100	12.28	0.29	-0.96
	beaming period-independent		
10	12.38	0.31	-1.42
100	12.20	0.27	-3.36

However, some information is lost when fitting only the B- and P- distributions, which are projections of the two-dimensional distribution of pulsars in the (B, P)-plane. A part of this information could be recovered by also fitting other projections, such as the distribution of the characteristic ages t_c. By deciding to omit the characteristic age from the search of the best solution, we have chosen to live with this disadvantage, in order to make sure that our measure of probability is not marred by the use of mutually dependent probabilities. For the same reason, we test for the product DM $\sin b$ rather than for the separate quantities DM and $\sin b$. Our definition of the Π that we try to maximize is arbitrary to some extent. However, we shall show below that a different choice would lead to the same overall conclusions.

In Fig. 4 we show the parameter area which gives the best solutions, for each of the five investigated values of τ separately. The maximum values of $\log \Pi$ reached in our simulations are shown in Table 1. Our most striking result is the dramatic increase in probability when the decay time is increased from 5 to 100 Myr. The difference in the quality of fit between 100 Myr and 300 Myr is insignificant. At long decay times the values of $\log B_0$ and σ_B for which the best solutions are reached are correlated.

We have also made contours of probability for χ^2 tests, and for $\Pi_5 \equiv \Pi \times Q_t$, where Q_t is the probability following from the K-S test on the distribution of t_c. The χ^2-probabilities vary only slowly over the parameter range in the $\log B_0$ - σ_B plane. For each decay time, they peak in the same area as the probabilities found with the Kolmogorov – Smirnov tests. The peak probability for a decay time of 10 Myr is virtually the same as that for 100 Myr. Due to their low sensitivity, the χ^2-tests do not discriminate between a long or a short time scale for field decay.

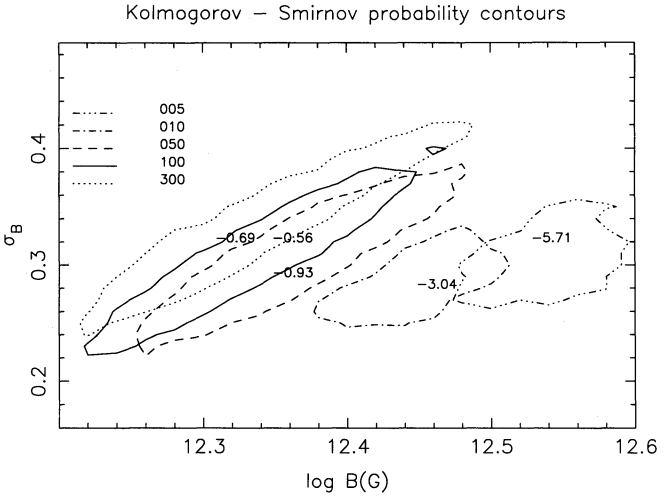

Fig. 4. Comparison of the areas in the $\log B_0$–σ_B-plane where the simulations give the best agreement with observations, according to the Kolmogorov – Smirnov tests, for different values of the decay time of the magnetic field. For each decay time, the contour is shown at which the probability is $1/e^2$ of the maximum probability obtained. The (logarithm of the) best probability is also indicated at the appropriate position. The long decay times consistently give higher probabilities than the short decay times

The highest Π_5 contours are almost coincident with the highest Π contours. The highest Π_5 values follow the same trend with decay time as the Π values, i.e. they increase between 5 and 100 Myr, and do not change significantly between 100 and 300 Myr.

3.2. Best simulations at 10 Myr and 100 Myr

To illustrate our results, we take a closer look at the best solutions for decay times of 10 and 100 Myr, respectively.

For the simulation with $\tau = 10$ Myr, the detection of 2000 pulsars required the input of 190 000 pulsars, 23 500 of which are still above the death line and beamed towards the Earth. To translate this into a birth rate, we note that the number of real pulsars observed in the four surveys is 130, and that the simulated pulsars were born in a time span of 50 Myr in a circle with radius of 3 kpc. (Because the normalization of the beaming in the simulation is the same as that for the real pulsars, i.e. $f_b \simeq 1$ at a pulse period $P = 0.1$ s, no further correction for beaming is required.) The birth rate in the circle is therefore $\simeq 250\,\mathrm{Myr}^{-1}$.

For the simulation with a decay time of 100 Myr, 770 000 input pulsars were required, of which 34 000 are above the death line and beamed towards the Earth. These pulsars were born in a time span of 300 Myr, hence correspond to a birth rate in the simulated circle of about $170\,\mathrm{Myr}^{-1}$, or about 2/3 of the birth rate in the simulation with $\tau = 10$ Myr.

These rates result in an overall galactic pulsar birth rate of about one per century, with the same large uncertainties as in previous studies.

In Fig. 5 we compare the distributions of age, magnetic field, and velocity in the z-direction, of the pulsars detected in the simulation, with the initial distributions given to the neutron stars at birth.

The top panels show that the pulsars that are detected are younger on average than the input population, and have lower magnetic fields. Several effects contribute to this result. Old pulsars, especially those with high initial fields, are likely to have

© European Southern Observatory • Provided by the NASA Astrophysics Data System

1992A&A...254..198B

evolved beyond the death line. The death line criterion therefore tends to remove such pulsars from the simulation sample. As pulsars with longer periods have smaller beams, the beaming further biases the age and field distribution towards small ages and low initial field strengths (because pulsars with low initial field strengths do not reach very long periods). These effects are counteracted to some extent by the higher mean luminosity of pulsars with strong magnetic fields. Because of the large spread in radio luminosities at each magnetic-field strength, luminosity selection of pulsars with strong magnetic fields is only a small effect, however.

The distribution of the magnetic-field strengths is shifted further towards lower field strengths due to field decay, as given by Eq. (1). As expected, this effect is stronger for the shorter decay times.

The bottom panels of Fig. 5 show that the v_z-distribution of the detected pulsars is narrower than that of the pulsars at birth. The reason for this is that pulsars with high velocities have moved to larger distances from the galactic plane — hence from the Sun — which reduces their radio flux observed at Earth and makes them more difficult to detect. For the short decay time of 10 Myr, gravitational deceleration has not had enough time to affect the pulsar velocities, and the observed velocity of each pulsar is close to its velocity at birth. In contrast, the detected sample of radio pulsars in the simulation with the longer decay time does contain pulsars that have been decelerated appreciably, including some that are moving back towards the galactic plane. In the simulation with $\tau = 100$ Myr, about 5 % of the detected pulsars at $\mathrm{DM} \sin|b| > 7.5\,\mathrm{cm}^{-3}\,\mathrm{pc}$ (i.e. outside the region where most pulsars are born) have velocities towards the galactic plane, whereas this fraction is 10 times smaller in the simulation with $\tau = 10$ Myr. Measurement of a sufficient number of pulsar velocities would thus provide a good indication of the decay time.

In Fig. 5 we compare the simulated with the real detected distribution of several pulsar properties, viz. the pulse period, the magnetic field, the "vertical component" of the dispersion measure, the radio luminosity, and the characteristic age. For these comparisons we use all 2000 simulated pulsars, multiplying the numbers in the histograms with 130/2000 to obtain the same normalization as for the real pulsars. The corresponding K-S tests are shown in Fig. 5. It is clearly seen from the irregular distributions of the real pulsars that they are much affected by Poisson noise, in contrast to the simulated distributions, which are much smoother. The simulations at both decay times produce too many pulsars at short periods. Due to the small numbers involved, this has little effect on the probability tests. In the simulation with $\tau = 10$ Myr, the period distribution is centered on shorter periods, and the magnetic-field distribution on higher fields, than the real pulsars. The $\tau = 100$ Myr simulation produces better P- and B-distributions. Both simulations do well in reproducing the distributions of the "vertical component" of the dispersion measure, and of the luminosity. Finally, the characteristic ages of the real observed pulsars are better reproduced by the simulation with the long decay time. The simulation with a short decay time produces pulsars with too low t_c on average, as is expected from the fact that the probability distribution of t_c can be shown to drop significantly for $t_c > \tau$.

To further illustrate the failure of simulations with short decay times, we compare the Kolmogorov-Smirnov tests for two different simulations with $\tau = 10$ Myr in Fig. 5. The figure shows that a better representation of the distribution of magnetic-field strengths can be obtained, by choosing a lower value for $\log B_0$, but only at the cost of the quality of the distribution of pulse periods. Conversely, a higher value for $\log B_0$ gives a better description of the period distribution, at the cost of a worse description of the B distribution.

The results of our comparison of the best solutions for $\tau = 10$ Myr with those of $\tau = 100$ Myr can be summarized as follows. The longer decay times lead to more pulsars at higher $|z|$, to some pulsars with velocities in the direction of the galactic plane, to a lower average magnetic-field strength at birth of neutron stars, to longer characteristic ages of the detected pulsars, and to a reduction in the required birth rate. The overall comparison suggests that the simulations with a longer decay time provide a better description of the statistics of real pulsars than the simulations with short decay times.

3.3. *Variation of other parameters*

While searching for the best solutions in the previously discussed simulations, we fixed the values of a number of model parameters, viz. the beaming and luminosity laws, the progenitor scale height, and the dispersion of the pulsar velocities at birth. We now briefly discuss the effect of varying these parameters.

The areas of best solutions shown in Fig. 4 show a correlation between the best values for B_0 and σ_B. The reason for this correlation is the relatively high number of observed pulsars with relatively low field, $\log B \sim 12$, which can only be reproduced with high values of B_0 if σ_B is sufficiently large. Apparently, a higher input at strong magnetic fields does not destroy the quality of the simulation. The reason for this is that most pulsars at high B quickly evolve to long pulse periods, where they are either beyond the death line, or have a high probability of being beamed away from the Earth. As only a few remain, they will on average be at large distance, and difficult to observe.

This latter effect shows up if we change the luminosity law used in the simulations from Eq. (10) to Eq. (11). The areas of best solution found with Eq. (11) include those found with Eq. (10), but extend to higher values of B_0 and σ_B. Already at a decay time of 10 Myr, the values of B_0 and σ_B for the best solutions are correlated. The extensions are possible because Eq. (11) does not increase the luminosity beyond a given maximum, thus allowing even pulsars with very strong magnetic fields to go undetected.

The effect of reducing the dependence on pulse period of the beaming factor, is to move the contours of best simulations towards lower values of $\log B_0$, and to increase (lessen) the probabilities at short (long) decay times (see Table 1). For beaming according to Eq. (6) the long decay time still gives better results than the short decay time. If the beaming is assumed not to depend on the pulse period, however, the short decay time gives better results. This is because both short decay times and period-dependent beaming laws reduce the fraction of high-field pulsars near the death line in the detected sample. It appears well established that the beaming factor depends on the pulse period (e.g. Lyne & Manchester 1988, Rankin 1990). Our conclusion that simulations with short decay times are not as successful as those with long decay times in reproducing the observed distributions of pulsar properties holds for the beaming laws of both Eq. (5) and Eq. (6).

All simulations produce too many pulsars at short periods. It appears possible then that some pulsars are born with pulse periods in excess of our minimum period. Because of the low sta-

© European Southern Observatory • Provided by the NASA Astrophysics Data System

1992A&A...254..198B

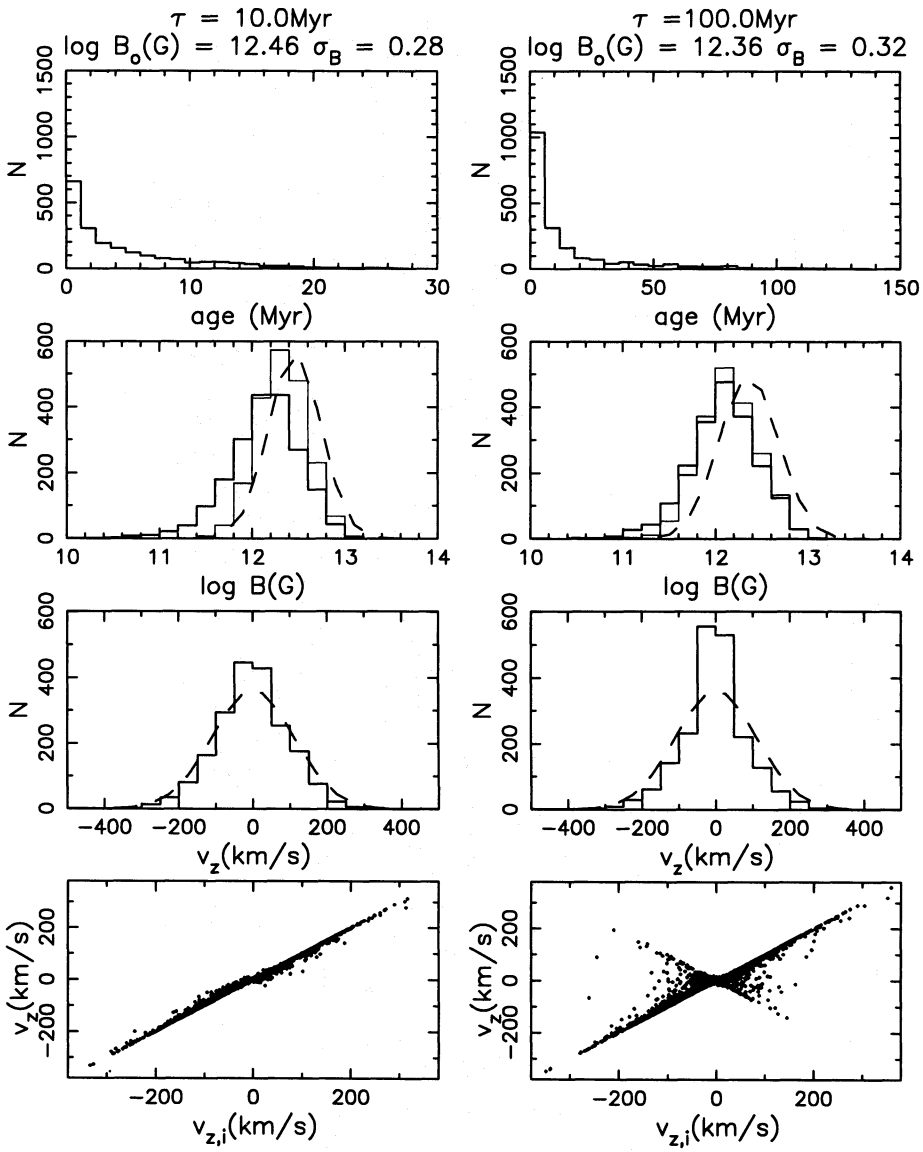

Fig. 5. Age, magnetic-field strength, and velocity distributions of radio pulsars detected in the simulations discussed in Sect. 3.2, for time scales for decay of the magnetic field of $\tau = 10$ Myr (left) and $\tau = 100$ Myr (right). The top panels show that the age distributions of the pulsars detected in the simulations peak toward short ages. For the magnetic fields we show the input distribution according to Eq. (1) (dashed), the initial distribution of the detected pulsars only (thin solid line), and the evolved distribution for the detected pulsars (thick solid line). The evolved velocity distributions (solid histogram) are narrower than the initial velocity distributions (dashed curves). In the bottom panels we plot the current velocity of the detected radio pulsars as a function of their initial velocity. The velocities of the radio pulsars in the simulation with a decay time of 10 Myr (left) have hardly changed in their short life. In contrast, radio pulsars in the simulation with a decay time of 100 Myr (right) may be old enough for their velocities to have changed markedly since their birth

tistical impact of the few pulsars at short periods, we refrained from actually testing different input distributions that include longer initial pulse periods. Such tests will only become meaningful once many more pulsars at short periods are discovered.

The scale height of the initial z-distribution of the radio pulsars is small with respect to the distance travelled during their characteristic life time. We expect therefore that the precise value of the scale height does not affect our results. Our simulations do not indicate a need for input at higher z, as found by Narayan & Ostriker (1990). The finite vertical extent of the electron layer does not lead to a second peak in the DM sin b distribution due to the pulsars at high z, but rather causes this distribution to drop less rapidly with increasing values. As shown in Fig. 5, the effect is not strong. In Fig. 5 we show the "vertical component" of the dispersion measure as a function of the real height above the galactic plane, for the detected pulsars in our best simulations at 10 and 100 Myr. The deviation of the relation between these quantities from a straight line shows the importance of the finite height of the electron layer. Our best simulation at 100 Myr indicates that about 10% of the 130 real pulsars in our comparison sample may be more than 1 kpc removed from the galactic plane.

The scale height of the observed radio pulsars depends also on the initial velocities that pulsars obtain at birth. To see how this affects our conclusion we have performed simulations in

© European Southern Observatory • Provided by the NASA Astrophysics Data System

1992A&A...254..198B

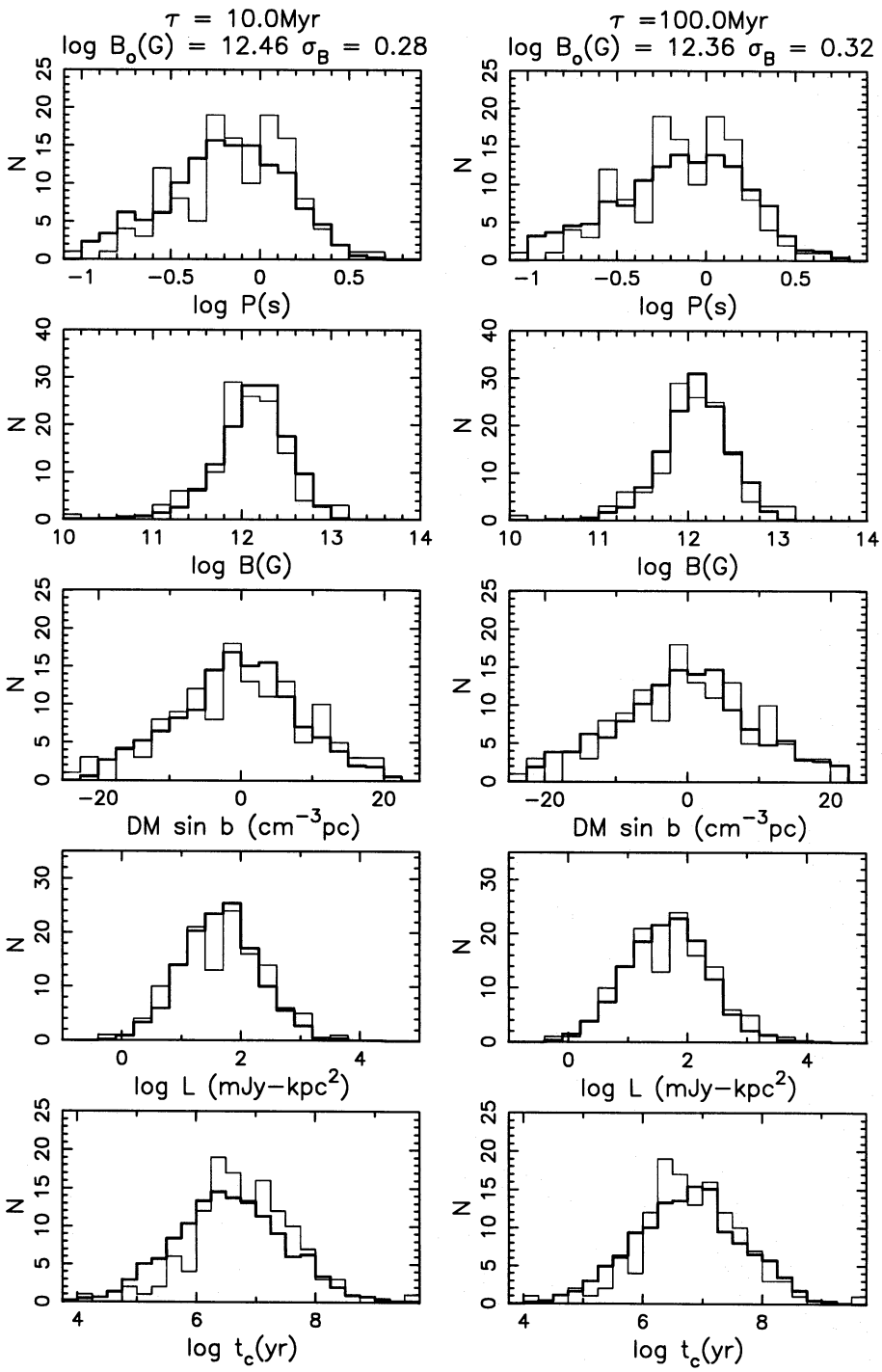

Fig. 6 Comparison of the distributions of (from top to bottom) pulse period, magnetic-field strength, "vertical component" of dispersion measure, radio luminosity, and characteristic age for simulated and real pulsars, for the best simulations with time scales for decay of the magnetic field of $\tau = 10$ Myr (left) and $\tau = 100$ Myr (right). The thin lines show the real pulsars, the thick lines the simulated pulsars. All 2000 simulated pulsars are used for the solid curves, but their numbers are normalized to the same total as the real pulsars by multiplication with 130/2000

which σ_v in Eq. (8) was taken to be 200 km/s. It should be noted that the acceleration in the z-direction given by Eq. (9) is only valid for distances to the galactic plane that are not too large. Our use of this equation at all z implies that even pulsars with velocities higher than the local escape velocity (~ 300 km/s) return to the galactic plane in our simulation. This could in principle cause problems for our simulations, but Fig. 5 shows that such high-velocity returning pulsars are not present in the detected sample.

In the simulations with $\sigma_v = 200$ km/s and $\tau = 100$ Myr, the location in the $\log B_0 - \sigma_B$ plane of the best simulations is not affected, but $\log \Pi$ drops by about 2. Some detected pulsars have high velocities, but virtually none of these are from pulsars returning from the apex of their orbit. A high velocity rapidly moves a pulsar to a large distance, where it easily escapes detection. In a simulation with $\sigma_v = 200$ km/s, the simulated detected pulsars are too young and have too short periods, as compared to the real detected pulsars. In addition, this simulation gives too many pulsars at high DM sin b. Our simulations therefore suggest that the average velocity with which pulsars move away from the galactic plane after birth should not be much in excess of 110 km/s.

© European Southern Observatory • Provided by the NASA Astrophysics Data System

1992A&A...254..198B

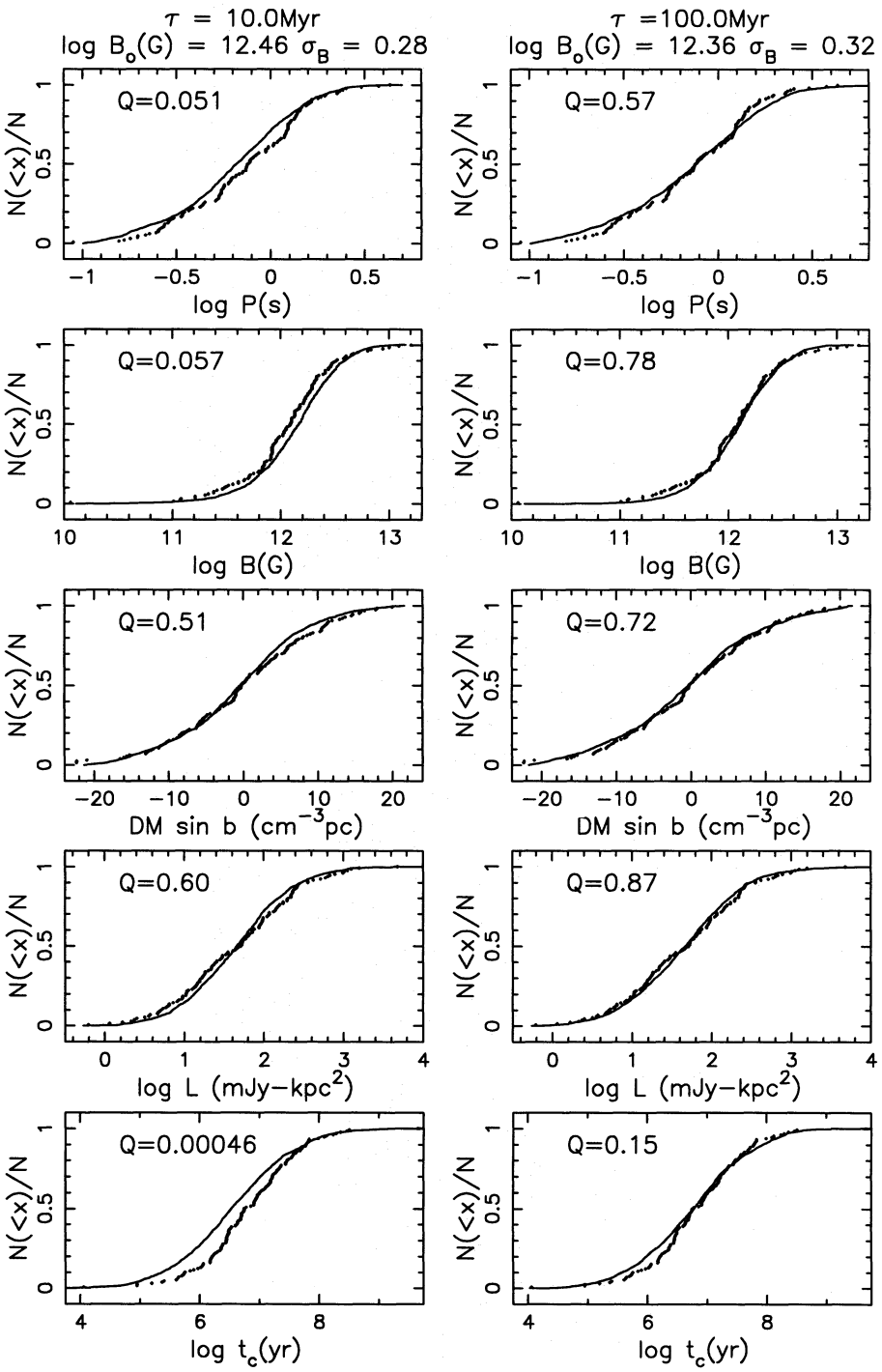

Fig. 7 Kolmogorov-Smirnov tests on the similarity between the distributions of (from top to bottom) the pulse period, magnetic-field strength, "vertical component" of dispersion measure, radio luminosity, and characteristic age for simulated and real pulsars, for the best simulations with time scales for decay of the magnetic field of $\tau = 10$ Myr (left) and $\tau = 100$ Myr (right). The dots show the individual real pulsars, the solid lines the simulated pulsars. Each graph is headed with the probability Q that the two distributions shown in the graph are drawn from the same population

The simulations with $\sigma_v = 200$ km/s and $\tau = 10$ Myr have the same problems as those with the longer decay time, except that the distribution of DM sin b improves with respect to the low-σ_v simulations. This improvement does not compensate, however, for the deterioration of the P- and t_c-distributions.

4. Discussion

The properties that we chose to use in searching for the parameters that lead to the best simulations are pulse period, magnetic-field strength, "vertical component" of the dispersion measure, and luminosity at 400 MHz. Of these properties, we find that DM sin b and L_{400} are well or moderately well reproduced by many of our simulations. These properties do not constrain the simulation parameters very much. P and B on the other hand are reproduced with greatly varying success as we vary the simulation parameters, and set good constraints on them.

As already discussed above, addition of the characteristic age to the properties that have to be reproduced by the simulation does not alter our results. The solutions that reproduce P and B well are also successful in reproducing t_c. We have made some further tests, and these show that the same is true for the period

© European Southern Observatory • Provided by the NASA Astrophysics Data System

1992A&A...254..198B

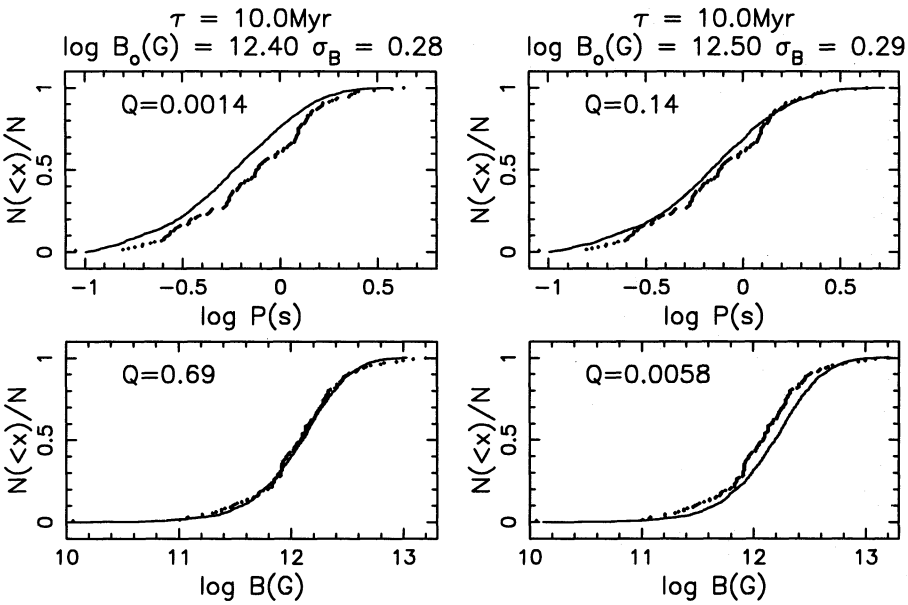

Fig. 8 Kolmogorov-Smirnov tests on the similarity between the distributions of the pulse period (upper panels) and the magnetic-field strength (lower panels) for simulated and real pulsars for two simulations with time scales for decay of the magnetic field of $\tau = 10$ Myr. As compared to the best fit at $\tau = 10$ Myr, the simulation on the left, for $\log B_0(G) = 12.40$ and $\sigma_B = 0.28$, gives a better correspondence for the observed magnetic-field distribution, at the cost of a worse distribution of pulse periods, whereas the one on the right, for $\log B_0(G) = 12.50$ and $\sigma_B = 0.29$, provides a better pulse period distribution, but a worse period distribution. The dots show the real pulsars, the solid lines the simulated pulsars. Each graph is headed with the probability Q that the two distributions shown in the graph are the same

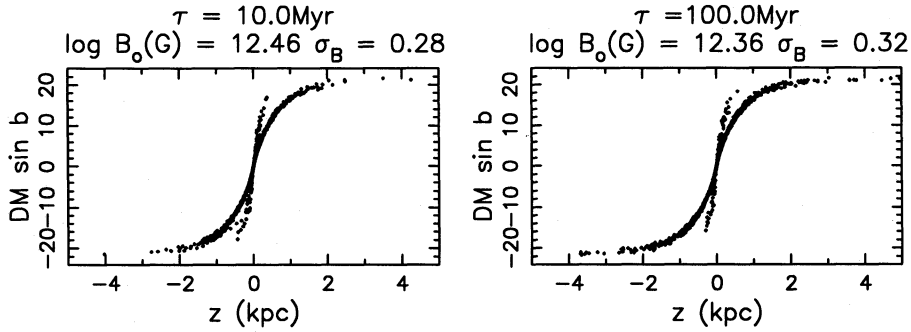

Fig. 9 DM sin b (in cm^{-3} pc) as a function of the height above the galactic plane z for the pulsars detected in our simulations with decay times for the magnetic field of $\tau = 10$ Myr (left) and $\tau = 100$ Myr (right). The pulsars behind the Gum Nebula follow a separate track. The finite height of the electron layer is visible in both simulations

derivative: our best solutions according to P and B also give better reproductions of the $\dot{P}$ distribution.

We have verified that our best simulations reproduce the distributions of DM and sin b separately in a satisfactory manner, in addition to the product DM sin b.

We may conclude that our result that high values of τ give better simulations does not depend on our choice of the properties that we have tried to fit.

If the decay time of the magnetic-field strength is short, the line in the $B - P$ diagram of a constant age of a few million years lies close to the death line. It has therefore been suggested that the observed death line may in part be due to the moderate age of most detected pulsars, in other words, due to selection effects favouring young pulsars (see for example Backer 1988 for a review). For long decay times, of ~ 100 Myr, we have found that many detected pulsars can be old enough to have crossed the position of the death line. This means that the death line cannot be due to selection effects, but must indeed represent a line beyond which the radio flux declines precipitously. Simulations in which we remove the death line constraint according to Eq. (13) do indeed lead to a large number of pulsars detectable to the right of and below the death line in the $B - P$ diagram. E.g., if we remove the death line constraint from our best simulation at $\tau = 100$ Myr, more than a fifth of all detectable pulsars are beyond the death line. Our result that long decay times give a better description of the observed pulsar population therefore implies that the death line is intrinsic to the emission mechanism, and not a selection effect.

Because our results seem to contradict conclusions reached earlier by other authors, we must explain how this can be the case. As explained in the introduction of our paper, selection effects have been taken into account by us more consistently than by

© European Southern Observatory • Provided by the NASA Astrophysics Data System

1992A&A...254..198B

most earlier authors. The dominant importance of selection effects therefore serves to explain the difference between our results and those of many earlier papers. Narayan and Ostriker (1990), however, do take into account selection effects consistently, and our description of most of them is in fact based on theirs.

The differences between our approach and those of Narayan and Ostriker are mainly: 1) our use of a more limited number of real pulsars, 2) our use of Kolmogorov - Smirnov rather than χ^2 tests, 3) our use of a finite scale height of the electron layer (see Eq. 16), and 4) the assumption by Narayan and Ostriker of two independent populations.

Our use of a smaller number of pulsars makes our comparison more sensitive to Poissonian uncertainties in the small sample of real pulsars. Because the Kolmogorov - Smirnov tests consistently favour simulations with long decay times, independent of variations in our other simulation parameters, we do not think that our selection of a smaller sample is the cause of our result. Our simulations show that a low value of the decay time τ makes a simultaneous good fit to both P- and B-distributions impossible. This conclusion in itself, in fact, is also drawn by Narayan & Ostriker, and causes them to include a second, independent population of radio pulsars. We do think that our use of Kolmogorov - Smirnov tests may make a difference, as these are more sensitive. On the basis of χ^2 tests we would not be able to express a preference for long decay times. We would find however, that long decay times are of equal quality. It is on the basis of the K-S tests that we find that long decay times provide better fits.

One of the reasons for us to start our investigation was the discovery that the electron layer has a finite extent from the galactic plane, and the determination of this extent with use of the pulsars in globular clusters (Bhattacharya & Verbunt 1991). We do indeed find that a good fraction of the detected pulsars are probably located well above the electron layer (see Fig. 5). We also find that reasonable fits to the "vertical component" of the dispersion measure DM $\sin b$ are found both at long and at short decay times, as shown in Figs. 5, 5.

The main difference between our results and those of Narayan & Ostriker is a consequence of their addition of a second population. We discuss this on the basis of Fig. 5, which shows that a single population does well in reproducing the B distribution, only at the cost of shifting the P distribution towards too short periods, if a decay time of 10 Myr is assumed. Fig. 5 also shows that a single population does well in reproducing the P distribution, at the cost of having too few pulsars with low magnetic-field strengths. Obviously, inclusion of a second population born with longer periods and lower field strengths can improve the correspondence between simulation and observations. The second population introduced by Narayan & Ostriker indeed is characterized by having longer initial spin periods.

Our simulations show that improvement is also possible by increasing the decay time of the magnetic field and simultaneously lowering the average pulsar field at birth. This is in apparent contradiction to the results found by Narayan & Ostriker (1990) in their simulation without field decay (their model r). We repeated our simulations with a scale height $H_2 = 6.8$ kpc, and find that long decay times are favoured even in this case. Thus, the contradiction cannot be attributed to our use of a different model for the electron density distribution. The extreme badness-of-fit for model r of Narayan & Ostriker is rather surprising to us. However, to investigate the cause of the contradiction we would need more details about the results of model r than are provided.

It is to be noted at this point that observations of pulsar velocities show a correlation between the magnetic-field strengths of pulsars and their velocities (Anderson & Lyne 1983; Cordes 1986; Harrison et al. 1991). We have, however, assumed no intrinsic relation between these quantities in our simulations. The results of our simulations do produce a weak $v - B$ correlation for the detected pulsars as a result of selection effects, but do not reproduce the observed degree of the correlation. However, the strength of the $v - B$ correlation for the observed pulsars has become somewhat weaker with the most recent measurement of pulsar velocities (Harrison et al. 1991), and the sample of pulsars for which this can be done is still fairly small. It is not clear, therefore, how representative the observed $v - B$ correlation is for the entire population, and we have chosen not to treat this aspect of the problem. It may well be that this correlation arises due to the special properties of a second population of pulsars which originate in binary systems (see, e.g. Bailes 1989; Bhattacharya & Van den Heuvel 1991), which cannot be accommodated in the form of a single homogeneous population of pulsars investigated in the present paper. However, as long as the fraction of the pulsars of this second category is small among the observed ones, it would not affect our conclusions to any noticeable degree.

5. Conclusions

The main conclusions of the present paper are the following:

1. Population syntheses with large (≥ 100 Myr) values for the time scale for the decay of the magnetic field of radio pulsars reproduce the properties of the observed radio pulsars much better than those with short decay times. This implies that there is no evidence for any significant decay of the magnetic field during the active life time of a pulsar.
2. It is important to take into account that the scale height of the galactic distribution of free electrons is finite. Our simulations show that more than 10% of the pulsars observed in 4 large surveys may be located more than 1 kpc away from the galactic plane.
3. In the future, measurement of a larger number of pulsar velocities will provide an additional powerful tool for the measurement of the time scale for field decay in single radio pulsars.

Acknowledgements. This work was supported in part by the National Science Foundation under grant No. PHY89-04035, supplemented by funds from the National Aeronautics and Space Administration, and by the Netherlands Organization for Scientific Research (NWO) under grants PGS 78-277 and SIR 13-602. Our work profited much from the good computing facilities at the Institute for Theoretical Physics. The figures in this paper were made with the packages SM, by P. Monger and R. Lupton, and PGPLOT, by T. Pearson.

We thank Rachel Dewey and Matthew Bailes for sharing their knowledge and some of their data with us, and for many discussions. Useful comments and suggestions by Don Backer and Roger Romani are gratefully acknowledged.

References

Anderson, B., Lyne, A.G., 1983, Nat 303, 597

Backer, D.C., 1988, in K.I. Kellerman and G.L. Verschuur (eds.), Galactic and Extragalactic Radio Astronomy, 2nd edition, Springer-Verlag, p. 480

© European Southern Observatory • Provided by the NASA Astrophysics Data System

1992A&A...254..198B

Bailes, M., 1989, ApJ 342, 917
Baym, G., Pethick, C., Pines, D., 1969, Nat 224, 673
Beskin, V.S., Gurevich, A.B., Istomin, Ya.N., 1984, ApSpSci 102, 301
Bhattacharya D., 1991, in J. Gil, T.H. Hankins and J. Rankin (eds.), Magnetospheric Structure and Emission Properties of Radio Pulsars, Pedagogical University of Zielona Gora press, Zielona Gora, Poland, in press
Bhattacharya D., Srinivasan, G., 1991, in J. Ventura and D. Pines (eds.), Neutron Stars: Theory and Observation, Kluwer Academic Publishers, Dordrecht, p.219
Bhattacharya, D., van den Heuvel, E.P.J., 1991, Physics Reports 203, 1
Bhattacharya, D., Verbunt, F., 1991, A&A 242, 128
Blair, D.G., Candy, B.N., 1989, in: Timing neutron stars, H. Ögelman and E.P.J. van den Heuvel (eds.), Kluwer, Dordrecht, p.609
Chevalier, R.A., Emmering, R.T., 1986, ApJ 304, 140
Cordes, J.M., 1986, ApJ 311, 183
Cordes, J.M., Weisberg, J.M., Boriakoff V., 1985, ApJ 285, 221
Damashek, M., Taylor, J.H., Hulse, R.A., 1978, ApJ 225, L31
Davies, J.G., Lyne, A.G., Seiradakis, J.H., 1972, Nat 240, 229
Dewey, R.J., Stokes, G.H., Segelstein, D.J., Taylor, J.H., Weisberg, J.M., 1984, in: Millisecond Pulsars, S.P. Reynolds, D.R. Stinebring (eds.), NRAO, p. 234
Emmering, R.T., Chevalier, R.A., 1989, ApJ 345, 931
Fokker, A.D., 1987, A&A 182, 41
Frail, D.A., Weisberg, J.M., 1990, AJ 100, 743
Gunn, J.E., Ostriker, J.P., 1970, ApJ 160, 979
Harrison, P.A., Lyne, A.G., Anderson, B., 1991, in E.P.J. van den Heuvel and S.A. Rappaport (eds.), X-ray Binaries and The Formation of Binary and Millisecond pulsars, Kluwer Academic Publishers, Dordrecht, in press
Haslam, C.G.T., Salter, C.J., Stoffel, H., Wilson, W.E., 1982, A&AS 47, 1
Hulse, R.A., Taylor, J.H., 1974, ApJ 191, L59
Krishnamohan, S., 1987, in D.J. Helfand and J.H. Huang (eds.), IAU Symp. 125: Origin and Evolution of Neutron Stars, D. Reidel, Dordrecht, p. 377
Kuijken, K., Gilmore, G., 1989a, MNRAS 239, 571
Kuijken, K., Gilmore, G., 1989b, MNRAS 239, 605
Kundt, W., 1988, Comm Astrophys 12, 113
Lyne, A.G., Anderson, B., Salter, M.J., 1982, MNRAS 201, 503
Lyne, A.G., Manchester, R.N., 1988, MNRAS 234, 477
Lyne, A.G., Manchester, R.N., Taylor, J.H., 1985, MNRAS 213, 613
Manchester, R.N., Lyne, A.G., Taylor, J.H., Durdin, J.M., Large, M.I., Little, A.G., 1978, MNRAS 185, 409
Mihalas, D., Binney, J., 1981, Galactic Astronomy, W.H. Freeman, San Fransisco
Narayan, R., 1987, ApJ 319, 162
Narayan, R., Ostriker, J.P.,1990, ApJ 352, 222
Narayan, R., Vivekanand, M., 1983, A&A 122, 45
Phinney, E.S., Blandford, R.D.,1981, MNRAS 194, 137
Press, W.H., Flannery, B.P., Teukolsky, S.A., Vettering, W.T., 1986, Numerical Recipes, Cambridge University Press
Proszyński, M., Przybycień, D., 1984, in: Millisecond Pulsars, S.P. Reynolds, D.R. Stinebring (eds.), NRAO, p. 151
Rankin, J.M., 1990, ApJ 352, 247
Rawley, L.A., Taylor, J.H., Davis, M.M., 1986, Nat 319, 383
Reynolds, R.J., 1989, ApJ 339, L29
Romani, R.W., 1990, Nat 347, 741
Ruderman, M.A., Sutherland, P.G., 1975, ApJ 196, 51
Sang, Y., Chanmugam, G., 1987, ApJ 323, L61
Sang, Y., Chanmugam, G., 1990, ApJ 363, 597
Shibazaki, N., Murakami, T., Shaham, J., Nomoto, K., 1989, Nat 342, 656
Slee, O.B., Dulk, G.A., Otrupcek, R.E., 1980, PASA 4, 100
Srinivasan, G., 1989, A&A Review, 1, 209
Srinivasan, G., Bhattacharya, D., Muslimov, A.G., Tsygan, A.I., 1990, Curr. Sci. 59, 31
Stollman, G.M., 1986, A&A 171, 152
Stollman, G.M., 1987, A&A 178, 143
Taylor, J.H., Manchester, R.N., 1977, ApJ 215, 885
Taylor, J.H., Stinebring, D.R., 1986, ARA&A 24, 285
Vivekanand, M., Narayan, R., 1981, JAA 2, 315

This article was processed by the author using Springer-Verlag LaTeX A&A style file 1990.

© European Southern Observatory • Provided by the NASA Astrophysics Data System